LYMPHATIC RESEARCH AND BIOLOGY
Volume 00, Number 00, 2018
© Mary Ann Liebert, Inc.
DOI: 10.1089/lrb.2018.0019

Development and Evaluation of a New *In Vivo* Volume Measuring System in Mouse Tail Lymphedema Model

Joonmyeong Choi, MS,[1,*] Kun Yung Kim, MD,[2,3,*] Jae Yong Jeon, MD,[4] Sung Hwan Yoon, MS,[5] Jung-Hoon Park, PhD,[5] Ho-Young Song, MD,[6] and Kyu-Jin Cho, PhD[1]

Downloaded by Seoul National Univ. Medical College from www.liebertpub.com at 12/23/18. For personal use only.

Abstract

Backgrounds: Secondary lymphedema is a common complication of parasitization and breast or gynecologic cancer therapy; however, options for the treatment of lymphedema are ineffective and limited. A mouse tail model is one of the most successful animal models for a lymphatic study. Lymphedema of the mouse tail is characterized by increases in the volume of the extremity caused by accumulation of tissue fluid, proliferation of fibroblasts and adipocytes, and excessive production of collagen. However, the study of lymphedema using mouse has been plagued with difficulty in directly assessing physiologic changes owing to limitations in the measurement of the mouse tail volume. Furthermore, the mouse tail volume cannot be obtained using the general *in vivo* measurement method such as volumetric water displacement.
Methods and Results: Lymphatic researchers have used the truncated cone formula to approximate the volume as used in the numerical approximation of a cylindrical figure. Although this formula is simple and easy to use, it has difficulties of repeatability and accuracy because the measurement procedure is highly subjective and the accuracy depends on the number of divided segments on the tail. In this article, two novel volumetric measurement methods for the mouse tail model were introduced. The methods were evaluated and compared using three mice with surgically created lymphedema on the tails.
Conclusions: The two continuous measuring methods showed a possibility to improve the conventional method by continuous measurement using visual and physical detecting methods. The proposed methods facilitate the extraction of longitudinal section-specific information, which can be an important clue in a lymphatic study.

Keywords: mouse tail model, evaluation technique of lymphedema, secondary lymphedema, *in vivo* volume measurement

Introduction

The lymphatic system plays a major role in maintaining tissue fluid homeostasis and contributes to immune surveillance by trafficking of lymphocytes and antigen-presenting cells to the lymph nodes. Dysfunction of the lymphatic system results in lymphedema.[1] In industrialized countries, it mainly occurs secondary to oncologic surgery and therapy by the disconnection of the lymphatic system. Currently, various treatment methods such as lymphovenous anastomosis or lymph node transplantation have been proposed; however, there is no definite treatment modality for secondary lymphedema.[2]

Animal models play an important role in basic research to understand the genetic and molecular cues. A mouse tail model is mostly used in secondary lymphedema research owing to the simplicity of the procedure and its effectiveness in producing lymphedema. Measurement of volume of an edematous tail is a basic method to evaluate the degree of secondary lymphedema.[3–13] The volume of a tail has been

[1]Biorobotics Laboratory, Department of Mechanical and Aerospace Engineering, Seoul National University, Seoul, Republic of Korea.
[2]Department of Radiology, Chonbuk National University Hospital, Jeonju, Republic of Korea.
[3]Research Institute of Clinical Medicine of Chonbuk National University, Jeonju, Republic of Korea.
[4]Department of Rehabilitation Medicine, Asan Medical Center, University of Ulsan College of Medicine, Seoul, Republic of Korea.
[5]Department of Biomedical Engineering Research Center, Asan Medical Center, University of Ulsan College of Medicine, Seoul, Republic of Korea.
[6]Department of Radiology, Asan Medical Center, University of Ulsan College of Medicine, Seoul, Republic of Korea.
*These authors contributed equally to this work and are cofirst authors.

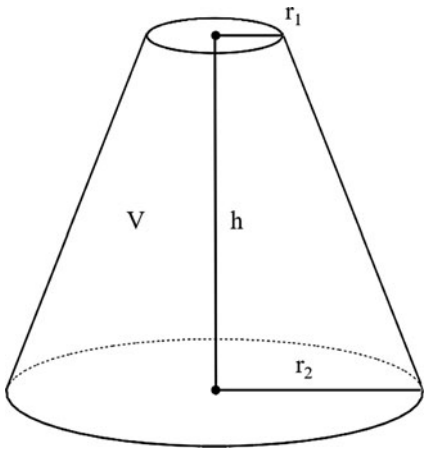

FIG. 1. Truncated cone. The volume of a truncated cone can be calculated using given lower and upper radii and height.

measured using several methods such as the truncated cone method, ultrasonography,[14] and optical three-dimensional sensor.[15] The truncated cone method is mostly used for measurement of a tail volume because it requires only a photograph of the mouse tail without the use of any special instrument. A mouse tail is divided into several truncated cones, and the total tail volume can be estimated by the sum of each truncated cone's volume.[16] However, this is based on the assumption that each truncated cone is a complete shape, which is hardly expected in a real *in vivo* experiment. Furthermore, it requires multiple measurements of the tail diameter at different sites, which is time consuming and subjective.

We propose the use of automatic processing to avoid random error from subjective measurement. Unlike the truncated cone method, the diameters and the area of various slices of a mouse tail can be digitally acquired such that the total volume of a tail can be calculated from the integral of the areas. To implement this method, our study proposed two techniques: semiautomated volume calculation using visual detecting software and automated volume calculation using a physical detecting device. Therefore, in this study, we assessed the tail volumes in a lymphedema mouse model, using each technique as well as the conventional truncated cone method.

Materials and Methods

Volume calculation by truncated cone method

The truncated cone formula was used to calculate the total volume of a mouse tail (Fig. 1). The usual formula for a truncated cone with upper radius r_1 and lower radius r_2 and height h is

$$V = \frac{1}{3}\pi h\left(r_1^2 + r_1 r_2 + r_2^2\right).$$

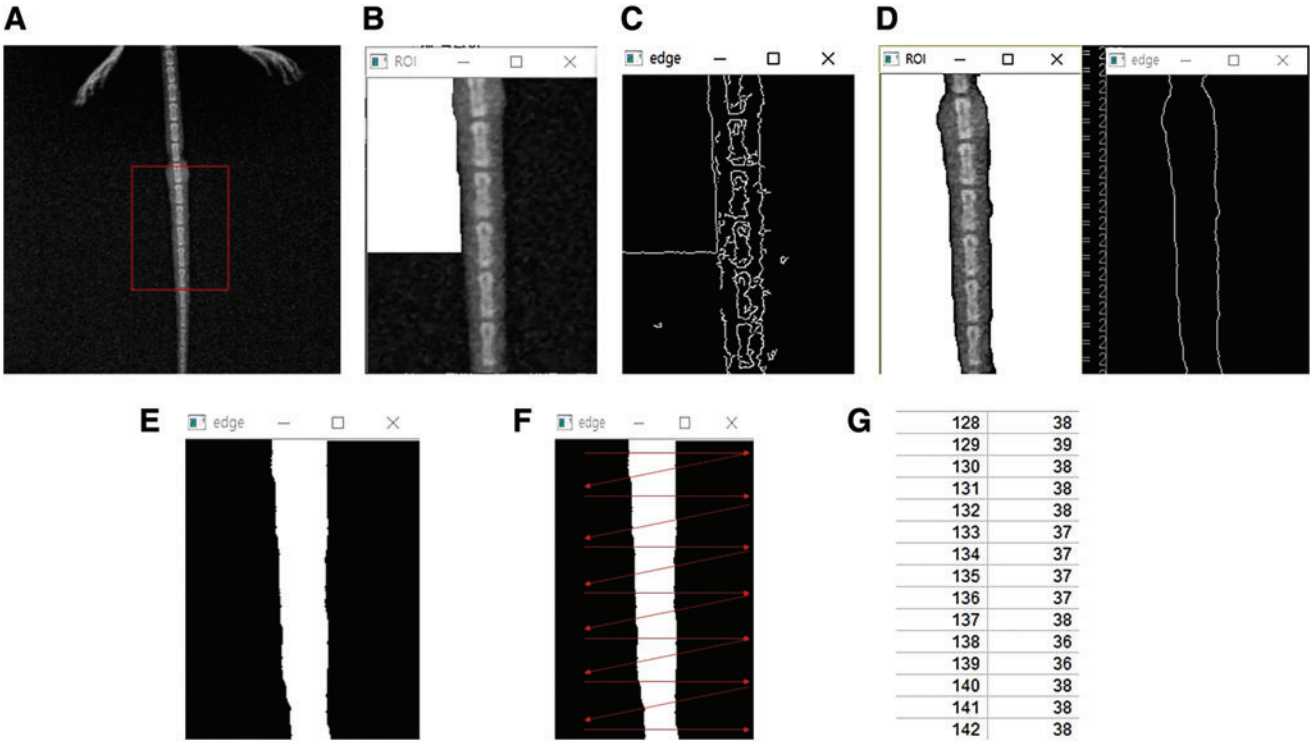

FIG. 2. Overview of the measurement process using visual detecting software. **(A)** The ROI in the main window was selected by a user. **(B)** The ROM (the contour line of tail surface) was selected by drag and drop action using a mouse in the ROI window. **(C)** After selecting the ROM from the ROI window, and the detected contour of the mouse tail was displayed in the ''edge'' window. **(D)** After selecting the ROM, the complete contour was displayed in ''edge'' window. **(E)** The inside of the contour will be filled with *white* pixels. **(F)** In the final step, selected image was scanned and the number of pixels in the horizontal direction was counted using a raster scan algorithm. **(G)** The program exported pixel values, which correspond to the actual scale as a text file. ROI, region of interest; ROM, region of measurement. Color images available online at www.liebertpub.com/lrb

Downloaded by Seoul National Univ. Medical College from www.liebertpub.com at 12/23/18. For personal use only.

Downloaded by Seoul National Univ. Medical College from www.liebertpub.com at 12/23/18. For personal use only.

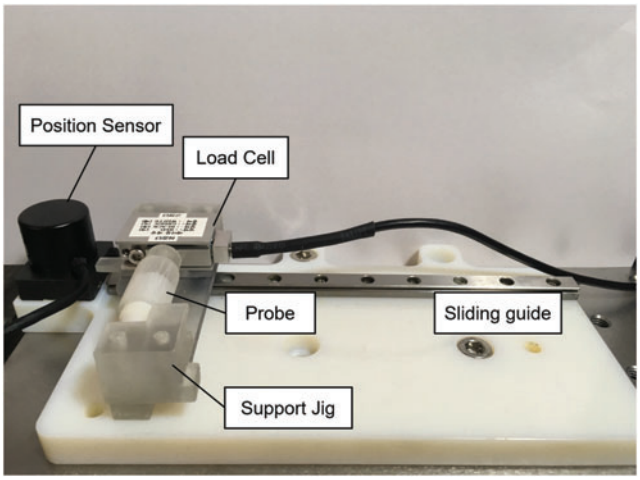

FIG. 3. Overview of physical detecting device. Color images available online at www.liebertpub.com/lrb

From this formula, the total volume V_{total} can be obtained from the sum of the respective volume of a cross section as follows:

$$V_{\text{total}} = \frac{1}{3}\pi \sum_{k=1}^{n+1} (h_{n+1} - h_n)\left(r_n^2 + r_n r_{n+1} + r_{n+1}^2\right).$$

Semiautomated volume calculation using visual detecting software

We developed a visual detecting software designed to determine the diameters of the entire tail. It contains a selection mode the region of interest (ROI), edge detection, selection of the region of measurement (ROM), noise removal, FloodFill, contour scanning, and exporting to text data. The software was programmed in visual studio 2010 platform with OpenCV 3.0. It can be run as a stand-alone application in Microsoft Windows 7 or later version.[17,18]

In the first step, the ROI in the main window was selected by a user (Fig. 2A). Next, the ROM (the contour line of tail surface) was selected by drag and drop action using a mouse in the ROI window (Fig. 2B). Canny edge detection method was applied to obtain a sharp outer line, which makes it easier to recognize the contour line of the mouse tail.[19] After selecting the ROM from the original image, the detected contour of the mouse tail was displayed in the ''edge'' window (Fig. 2C). After selection of the ROM, two thresholds were used to remove noise inside and outside the ROM. If a pixel gradient is higher than the upper threshold, the pixel is accepted as an edge. If the thresholds are appropriately selected, the contour of the mouse tail will be obtained (Fig. 2D). The ''FloodFill'' function in OpenCV library was used to fill the inside of the contour with white pixels (Fig. 2E). To facilitate diameter measurement in the X–Y plane, counting pixels and unit conversion were done automatically by the program in the contour scanning process. In the final step of visual detection, the selected image was scanned and the number of pixels in the horizontal direction was counted using a raster scan algorithm (Fig. 2F). When scanning is completed, the program exported pixel values, which correspond to the actual scale as a text file (Fig. 2G). The values were recalculated into the millimeter scale in this process. The volume was calculated by employing the aforementioned formula using a data processing code developed in a numerical computing environment (Matlab; MathWorks, Inc., MA).

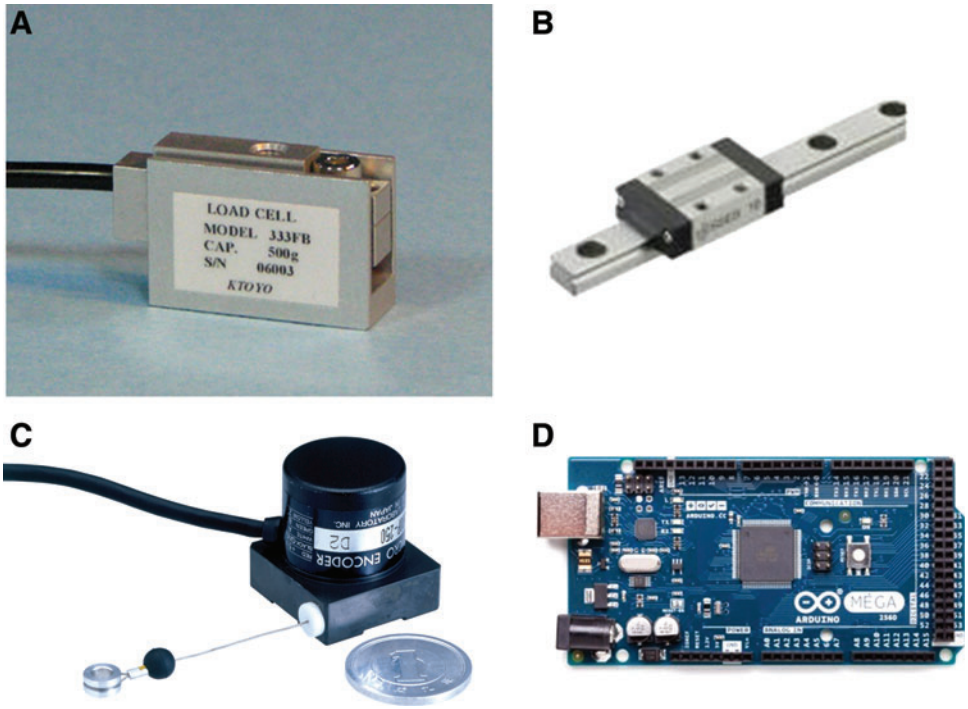

FIG. 4. Components of the physical detecting device. **(A)** A load cell with measuring range of 0.005–200 g. **(B)** A linear guide with a length of 150 mm. **(C)** A wire type linear scale with a resolution of 0.04 mm. **(D)** A microcontroller. Color images available online at www.liebertpub.com/lrb

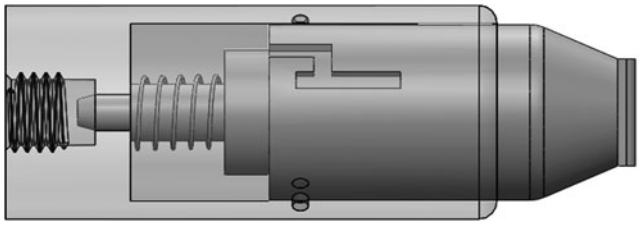

FIG. 5. Probe design for physical contact detection. The spring surrounded by jig wall can only generate a one-way linear motion. The measuring head that attached to the spring tip has a cylinder shape.

Automated volume calculation using the physical detecting device

We developed a physical detecting device for automated volume measurement as shown in Figure 3. The measurement instrument consisted of a probe, a load cell with measuring range of 0.005–200 g (Fig. 4A), a linear guide with a length of 150 mm (Fig. 4B), a wire type linear scale with a resolution of 0.04 mm (Fig. 4C), and a micro controller (Fig. 4D). The probe includes a coil spring with a spring constant of 0.098 N/mm, a supporting shaft, and sliders (Fig. 5). The operating principle of the device is based on Hooke's law, which describes the relationship between force and the extension of a spring. We used a 3D-printed (CONNEX 260; Stratasys Ltd., MN) jig, which generates a one-way linear motion according to Hooke's law, to measure the diameter of the mouse tail. The head part attached to the spring tip had a half-cylindrical shape. The probe consisted of a jig and a head part, and was moved along the linear rail to scan the entire mouse tail diameter. A load cell on the linear rail was aligned to measure the lateral forces. The complete mechanical components and sensors were fixed on a sensor manifold and wired as an independent system (Fig. 6).

The force (F) required to compress a spring is linearly proportional to the compressed distance of the spring (x) ($F = kx$). F can be obtained from a load cell, whereas x is constant. Therefore, the change in x at every slice through the mouse tail can be calculated from the formula. The specific information of components in the measuring instrument is shown in Table 1.

The experiment was conducted using a tapered object (Fig. 7A) to verify the repeatability and linearity of the physical detecting device. The graph in Figure 7B shows the correlation between experimental results and original data; however, the original dimensions had a slightly more acute angle. From several trials, a minimum error of 0.57% was obtained for physical detection.

In vivo *experimental protocol*

To compare the conventional and proposed methods, an experimental protocol was designed using a mouse tail lymphedema model. Tail lymphedema was created in three 10- to 12-week-old female C57BL/6 mice (Orient Bio, Seong-nam, Korea). The mice were anesthetized with an intramuscular injection of 50 mg/kg zolazepam and tiletamine (Zoletil 50; Virbac, Carros, France) and 10 mg/kg xylazine (Rompun; Bayer HealthCare, Leverkusen, Germany), and the skin was circumferentially excised 18 mm distal to the base of the tail, making a 2 mm circular band. The lymphatic collecting vessels were cauterized using the Bovie cautery.[20]

The tail diameter and volume were measured before surgery, 3.5 days, and 7 days after the surgery. Photographs were taken using a Canon D550 camera mounted on a tripod. The tail diameter measurement and volume calculation were made from these digital images using an image processing software (ImageJ; U.S. National Institutes of Health, Bethesda) and the developed visual detecting software. The physical detecting device was used to measure the volume of the tail. The images used in every visual detecting method have 4572×3168 pixels resolution. Detailed description and technical information for ''Materials and Methods'' was provided in Supplementary Data (Supplementary Data are available at www.liebertpub.com/lrb).

Results

The animal experiments were conducted based on the designed protocol to assess the developed visual detecting

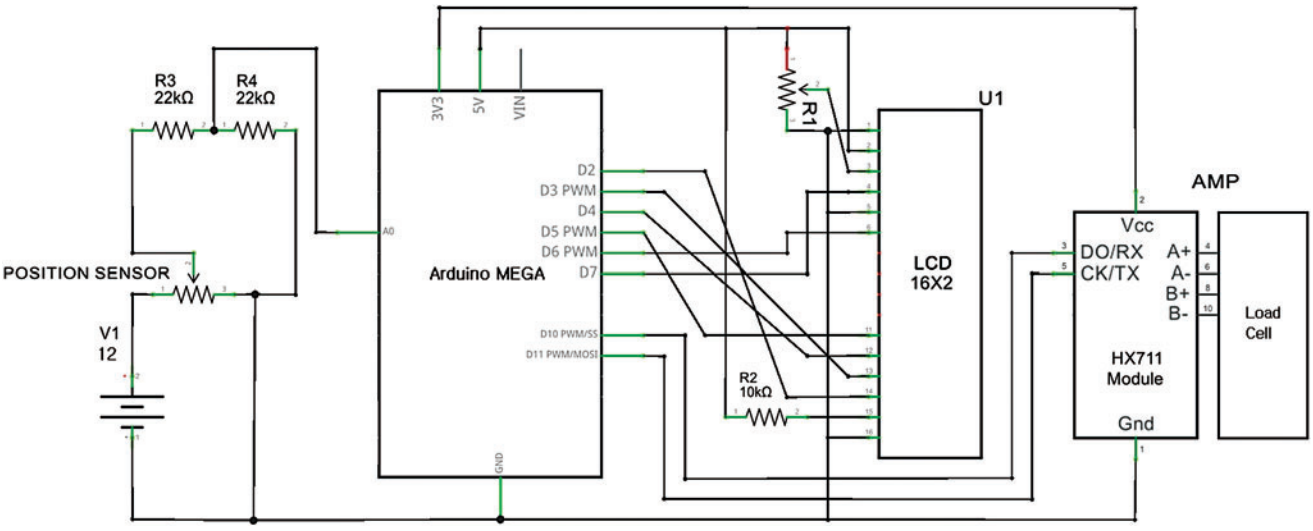

FIG. 6. Circuit diagram of the physical detecting device. Color images available online at www.liebertpub.com/lrb

Downloaded by Seoul National Univ. Medical College from www.liebertpub.com at 12/23/18. For personal use only.

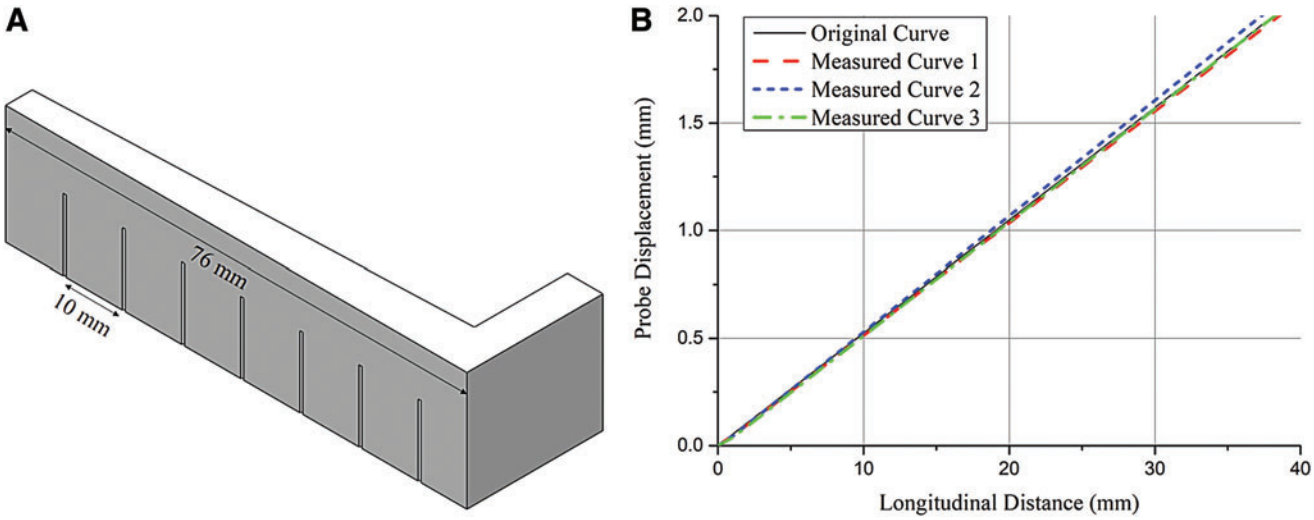

FIG. 7. Linearity verification of the physical detecting device. **(A)** A tapered object that was designed to verify the repeatability and linearity of the physical detecting device. **(B)** The result shows the correlation between experimental results and original data. Color images available online at www.liebertpub.com/lrb

software and physical detecting device. In terms of the measuring sequence, three types of methods were compared: (1) conventional method of measurement using image processing software, (2) proposed measurement method using the developed visual detecting software with OpenCV, and (3) another proposed measurement method using the developed physical detecting device. As shown in Figure 8A and B, a photograph was obtained at every measurement. Figure 8C shows the experimental setup using the physical detecting device. Every measurement was made 0 to 60 mm from the base of the tail in the longitudinal direction.

Figure 9 shows the measurement data using ImageJ in which the longitudinal distances correspond to the tail diameter in the three experimental mice. Every measurement was made at every 10 mm from the tail base. It can be observed

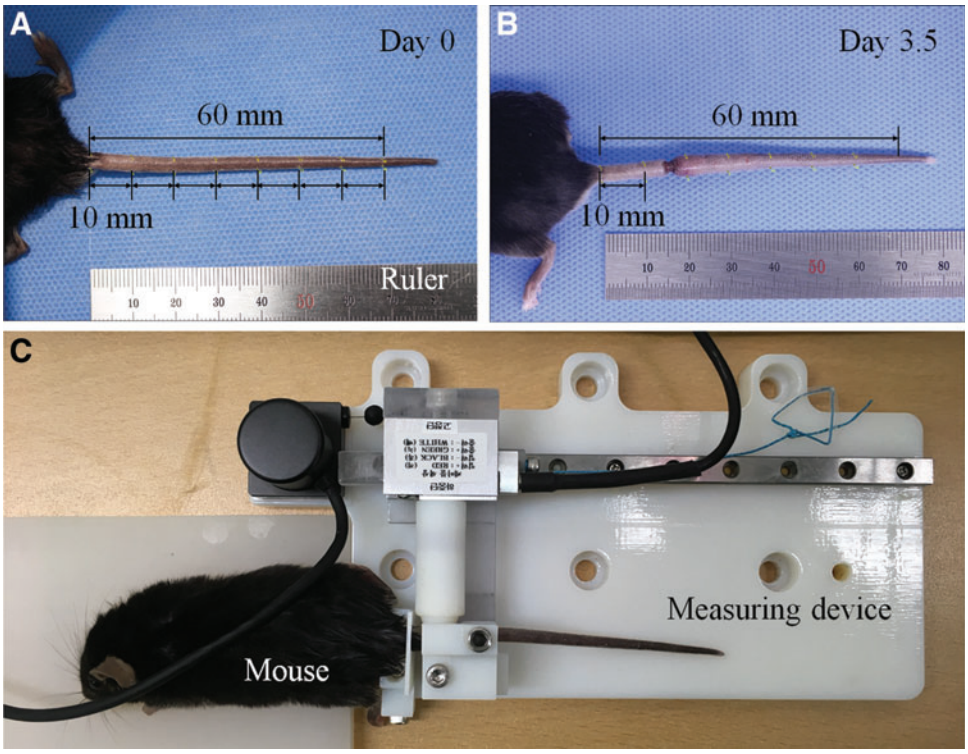

FIG. 8. Experimental scene using the mouse. **(A)** A photograph was taken by a camera before lymphedema surgery. **(B)** The lymphedema was observed near the surgical site a few days later. **(C)** The experimental setup using the physical detecting device. Color images available online at www.liebertpub.com/lrb

Downloaded by Seoul National Univ. Medical College from www.liebertpub.com at 12/23/18. For personal use only.

Downloaded by Seoul National Univ. Medical College from www.liebertpub.com at 12/23/18. For personal use only.

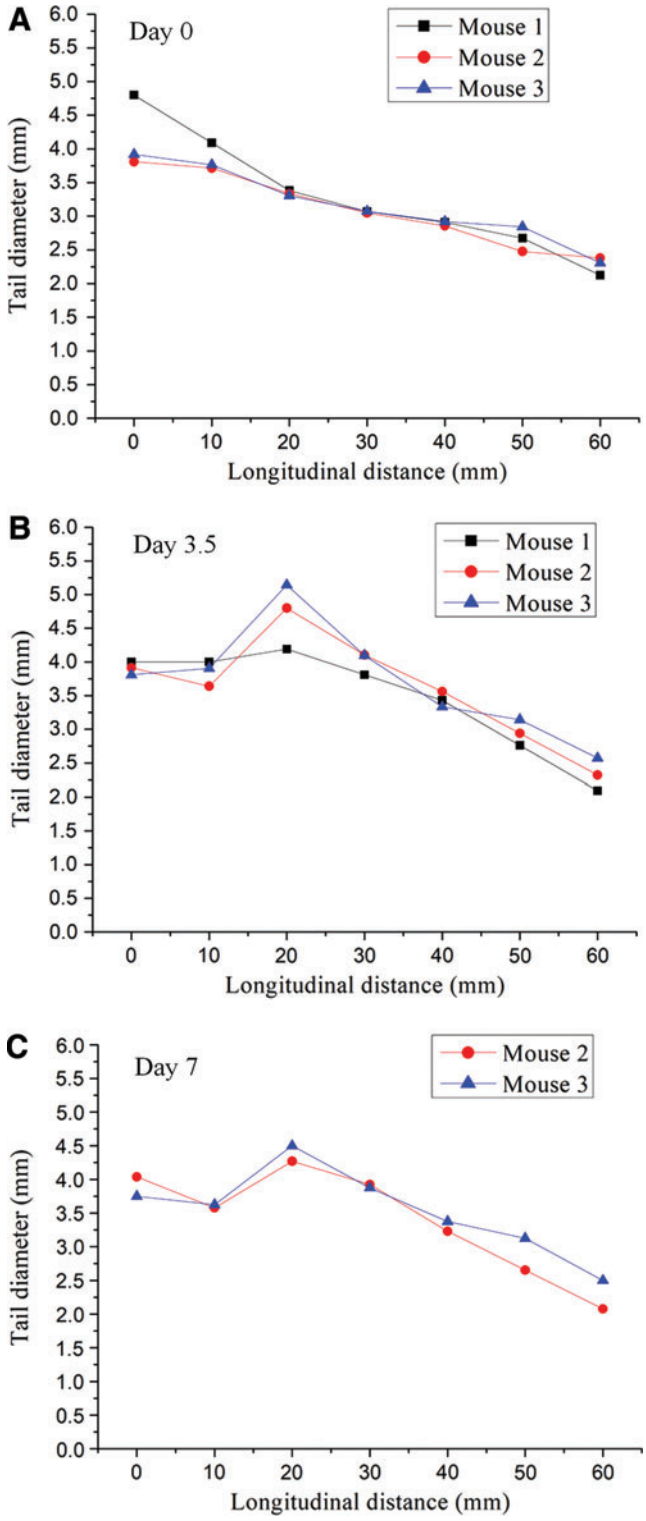

FIG. 9. Measurement results of the tail diameter using ImageJ. **(A)** Measurement results before lymphedema surgery. **(B)** Measurement results 3.5 days after lymphedema surgery. **(C)** Measurement results 7 days after lymphedema surgery. Color images available online at www.liebertpub.com/lrb

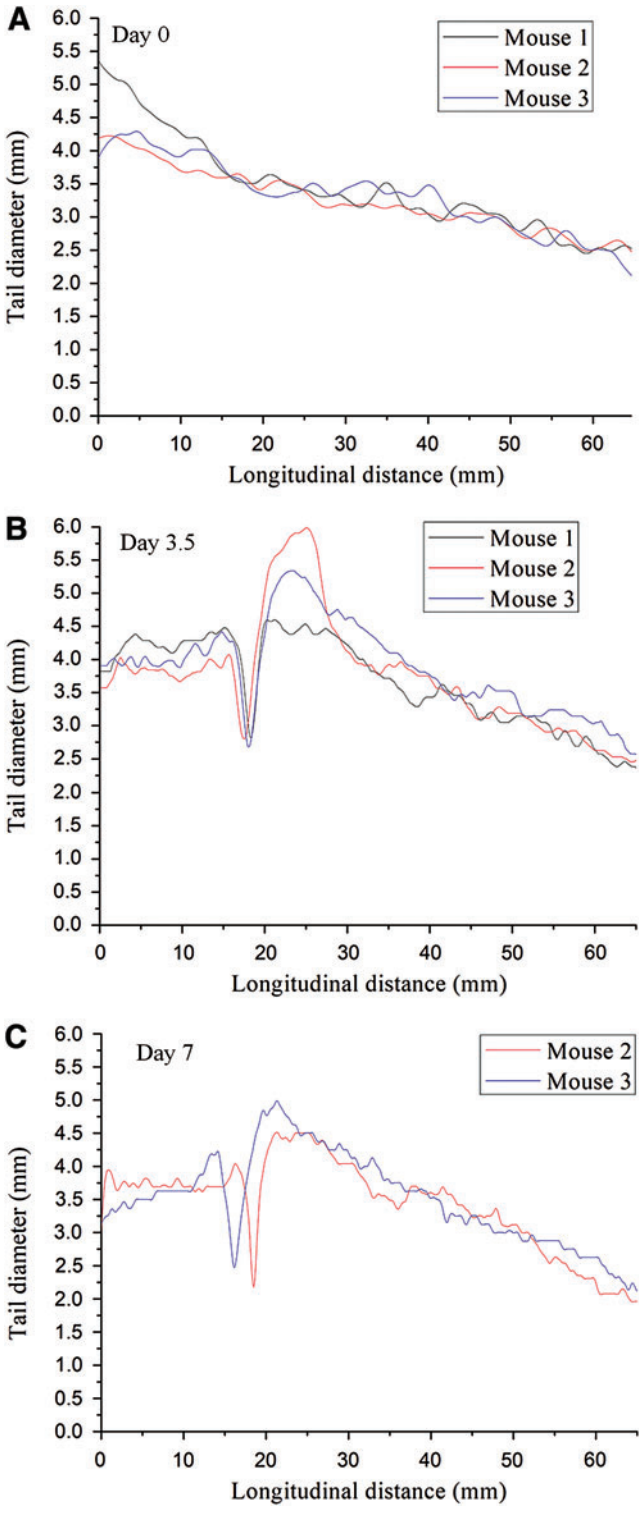

FIG. 10. Measurement results of the tail diameter using the developed visual detecting software. **(A)** Measurement results before lymphedema surgery. **(B)** Measurement results 3.5 days after lymphedema surgery. **(C)** Measurement results 7 days after lymphedema surgery. Color images available online at www.liebertpub.com/lrb

Downloaded by Seoul National Univ. Medical College from www.liebertpub.com at 12/23/18. For personal use only.

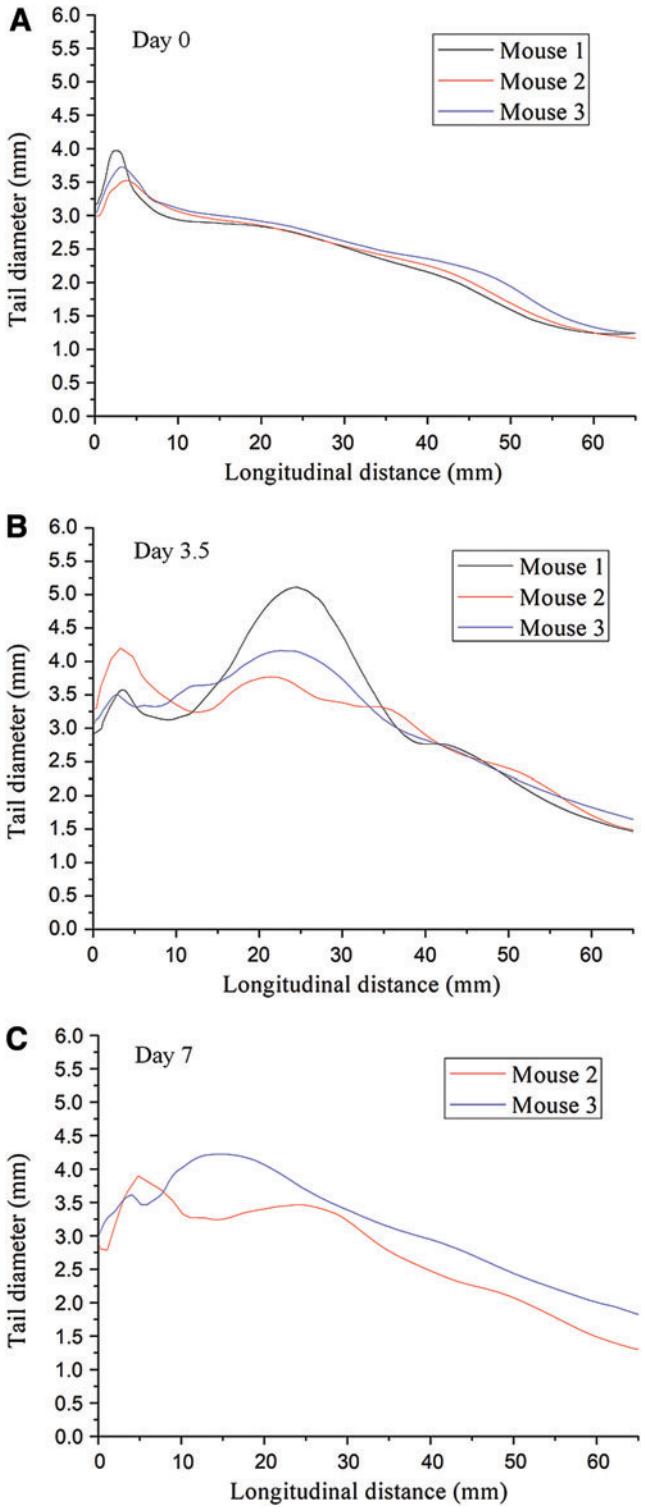

FIG. 11. Measurement results of the tail diameter using the developed physical detecting device. **(A)** Measurement results before lymphedema surgery. **(B)** Measurement results 3.5 days after lymphedema surgery. **(C)** Measurement results 7 days after lymphedema surgery. Color images available online at www.liebertpub.com/lrb

from the graph that there is a little negligible individual difference in each mice diameter. The maximal diameter of the tail reached the maximum value 3.5 days after surgery. The maximal diameter was mostly observed at 20 mm from the beginning of the tail. After 7 days, the maximal diameter showed a tendency for gradual reduction. Mouse 1 died after the second measurement due to postoperative complications.

The measured data using the visual detecting software with OpenCV showed intermittent perturbations (Fig. 10). These could be due to the effect of manual operation of the measuring area on the images. Furthermore, the contour of the tail was ambiguous due to the presence of fur. However, the results showed the same tendency as the image processed data. With an appropriate unit translation from pixel to millimeter unit, the smallest value representable is 0.02 mm. In the first experiment, the tail base diameter of mouse 1 was slightly larger than that of others, and it gradually decreased along the longitudinal axis. After 3.5 days, surgical lymphedema was clearly observed adjacent to the surgical site. Surgical lymphedema is represented as peak to valley.

The physically measured data denoted the smallest values in all measuring methods (Fig. 11). The change in volume at surgical site due to surgical lymphedema was significant after 3.5 days. Overall, the total volume expansion due to lymphedema decreased after 7 days. From the follow-up after 7 days, the decrease in tail volume may be because of necrosis in all mice tails.

Three methods were compared using the measured data (Fig. 12). The image-based methods and the physical detection method showed differences in volume. Overall, the results from the physical detection method showed a tendency for lower values compared with the other methods. The most noticeable difference among the methods was observed in the range of 20–40 mm from the beginning of the tail after 3.5 days. The total volume change by a measuring method was compared to correlate the measured data (Fig. 13).

Conclusions

Difficulties in the quantitative assessment of a mouse tail lymphedema model are mainly due to its small size. Circumferential diameter measurement, water displacement, and scanning with a perometer are commonly used in the measurement of the degree of lymphedema in humans. However, these methods cannot be applied to a mouse tail lymphedema model. Although the usefulness of measurement using microcomputed tomography in a mouse limb model has been reported,[21] its use in a daily experimental setting is not practicable owing to its complexity.

Most previous studies on the mouse tail lymphedema model used the truncated cone method to measure the tail volume. In this method, a mouse tail is divided into four or five segments of a truncated cone, and the sum of each truncated cone volume is calculated mathematically. This method does not require any special instrument, rather, it uses only a photograph of the entire tail; thus, it is one of the simplest methods of measuring entire tail volume. However, it does not reflect the exact geometry of the mouse tail because it assumes that each truncated cone is a perfect shape. If the number of calculated segments is increased, the calculated volume can be approximated as a real volume.

Downloaded by Seoul National Univ. Medical College from www.liebertpub.com at 12/23/18. For personal use only.

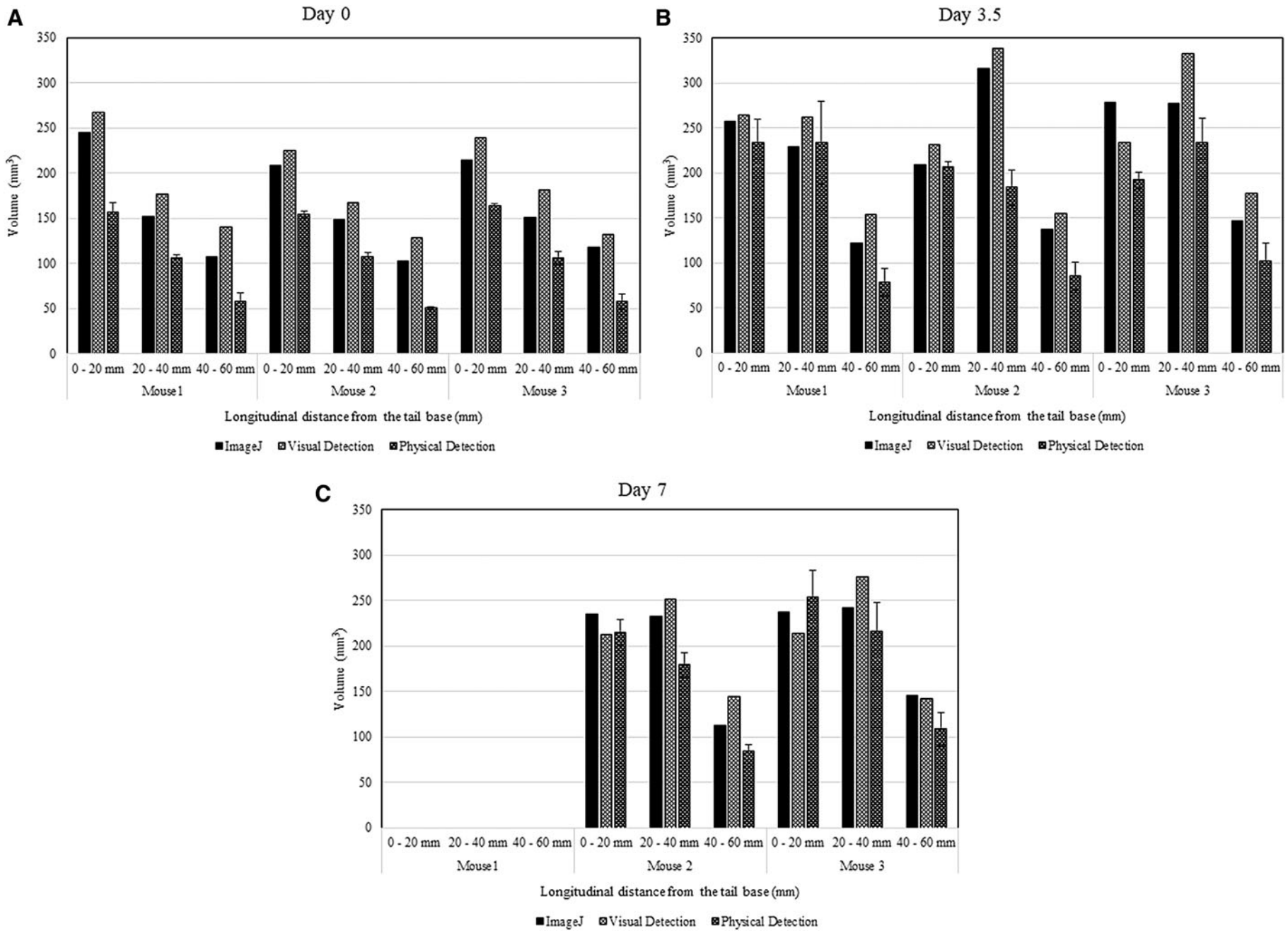

FIG. 12. Comparison of the differential tail volume using three methods. **(A)** Measurement results before lymphedema surgery. **(B)** Measurement results 3.5 days after lymphedema surgery. **(C)** Measurement results 7 days after lymphedema surgery.

Downloaded by Seoul National Univ. Medical College from www.liebertpub.com at 12/23/18. For personal use only.

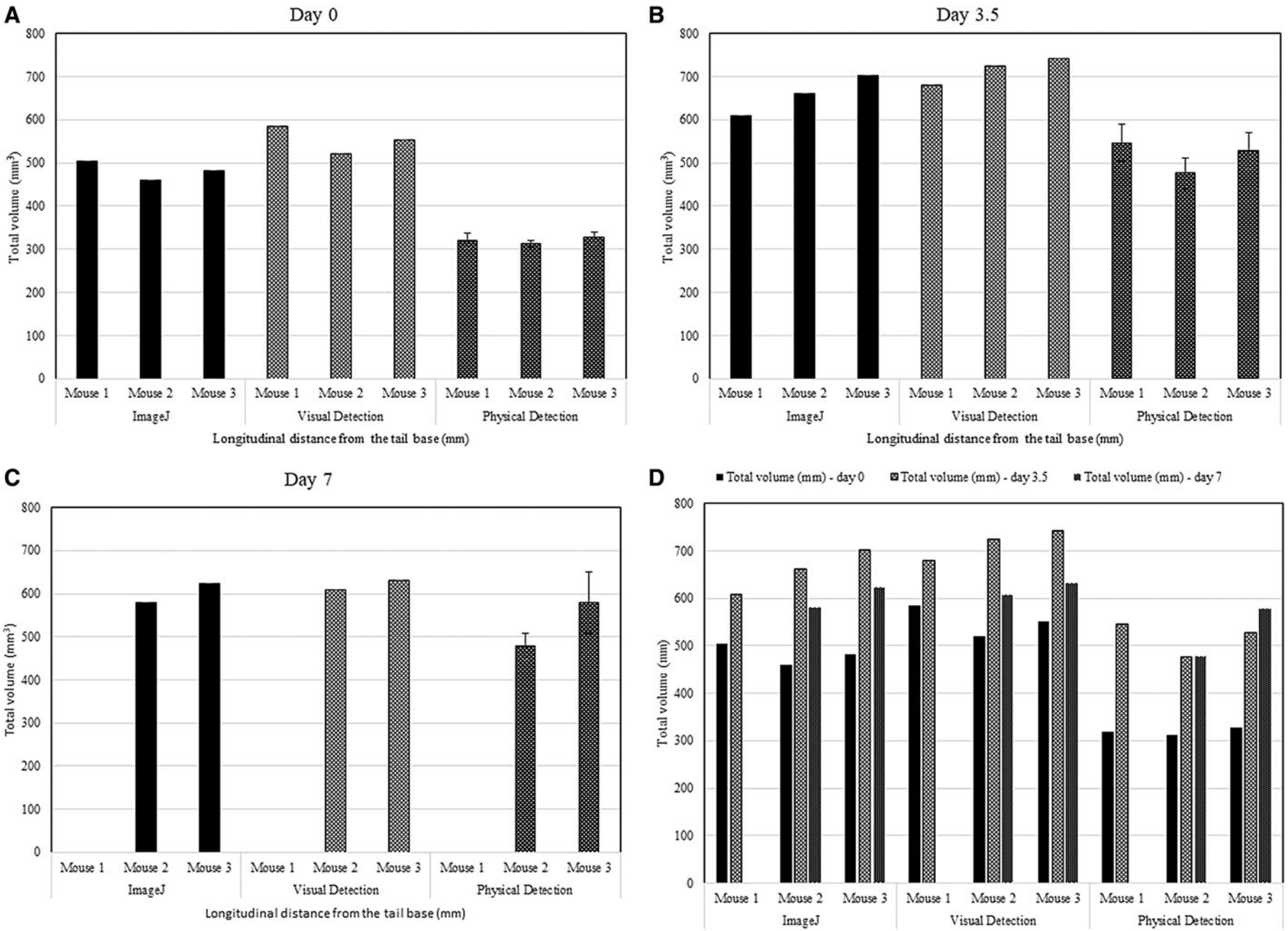

FIG. 13. Comparison of the total tail volume using three methods. **(A)** Measurement results before lymphedema surgery. **(B)** Measurement results 3.5 days after lymphedema surgery. **(C)** Measurement results 7 days after lymphedema surgery. **(D)** Total volume by time point.

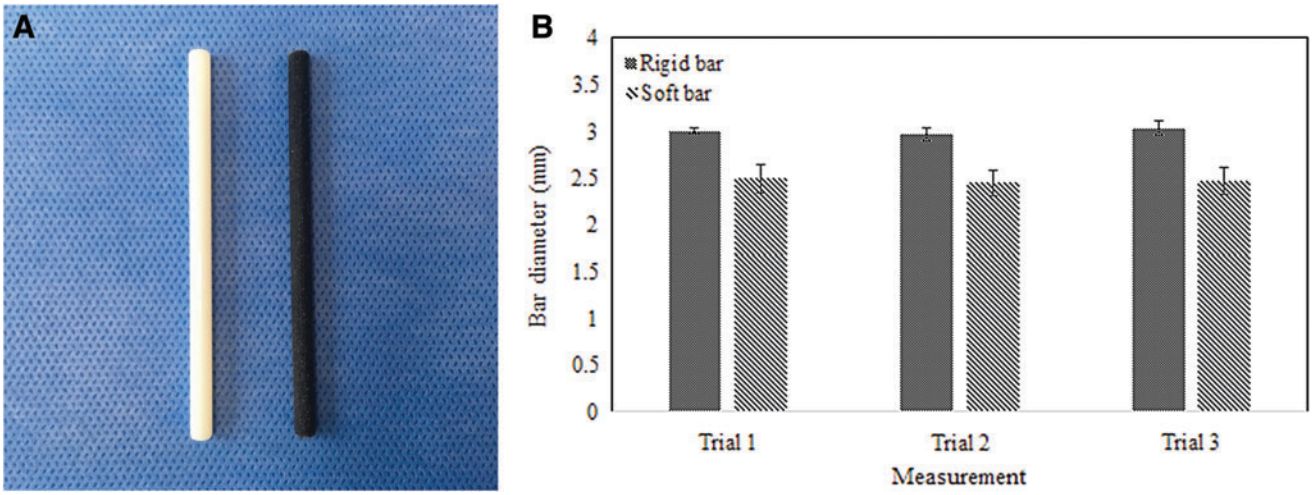

FIG. 14. Verification of a measuring error by skin deformation during physical detection. **(A)** The bars were made of two 3D-printed materials: rigid (*left*) and rubber-like soft (*right*). **(B)** Measurement results of two types of bars using physical detecting device. Color images available online at www.liebertpub.com/lrb

However, the measurement of tail diameter at multiple points is time consuming and increases random error.

To overcome the limitations of the conventional truncated cone method and to determine the volume of a mouse tail with high accuracy and convenience, two novel *in vivo* measuring methods were proposed in our study: semi-automated volume calculation using visual detecting software and automated volume calculation using a physical detecting device. The first method gives the exact geometry of the mouse tail. Dedicated visual detecting software was designed, and edge detection and contour detection algorithms were easily implemented on the experimental image based on the C++ platform with OpenCV. However, it is still time consuming as it requires a fastidious manual outline drawing. The second method gives the geometry of the mouse tail by sensing the force applied to a spring, thereby minimizing manual work and time. The physical contact-based diameter-measuring device was designed and built. Its principle of operation is based on a simple formula derived according to Hooke's law. The device was designed as a dedicated data acquisition system for cone-shape diameter with several moving components and sensors.

The results of our study indicate that there were some volume differences in the three methods. The main reason for the differences between visual detection and physical detection methods is possibly due to skin deformation. Our results show that skin deformation during measurement was not negligible in a normal and lymphedematous tail. To investigate an effect of skin deformation, additional experiment was conducted. The experiment was designed to show an error due to skin deformation of a mouse tail using cylindrical bars. The bars were made of two 3D-printed materials: rigid and rubber-like soft (Fig. 14). From the result, skin deformation cannot be compensated in physically measured data because there is no information of flexibility of each mouse tail. However, using visual detection and physical detection, geometric differences can be combined as single data to obtain a stiffness information of the localized section on the mouse tail. A spring in the probe can be changed to apply a different force to the tail surface. Because the localized tissue swelling has possibilities to affect a flexibility change, this will be a possible advancement of the proposed method.

Table 1. Components of the Measuring Instrument

Component	*Manufacturer/model number*
Wire type linear scale	MTL/MLS-12-1500-250
Coil spring	MISUMI/UY4-5
Linear guide	MISUMI/SSEBL8-150
Ball roller set screw type	MISUMI/BCSB6
Miniature ball guide set	MISUMI/BYHZ2-30-10-10
Load cell	KTOYO/333FB
Micro controller	Arduino MEGA/many

One concern in the automated volume calculation using a physical detecting device is the deformation of the skin by the compressive force of the spring. Although the spring constant of the probe is extremely low, the surface condition can increase or decrease the detected force. This might be attributed to an acute angle near the surgical site. When the probe contacts the tissue interface of those portions, the influence of the maximum static frictional force between the tissue and probe surface seemed dominant. To calibrate an offset error of the physical detecting device, a cylindrical rigid rod with a diameter of 3 mm was used before each measurement. Furthermore, the friction at the contact point can affect the measuring result; therefore, all measurements were made at a constant travel speed. If a travel speed of the probe along the linear guide exceeds 3 mm/s, the data acquisition was set up to be stopped. The method was helpful to suppress the fluctuation of the data by a dynamic friction.

The error in measurement using physical detecting device is also affected by a nonlinearity of the spring in the probe. When the deformation of a spring exceeds 4.5 mm, an effect of nonlinearity on the measurement can be prominent. The linear elastic range of the spring in the probe is up to 4 mm. This could be solved by an experimental setup with an appropriate offset value. If the surface condition is dominant in

Downloaded by Seoul National Univ. Medical College from www.liebertpub.com at 12/23/18. For personal use only.

physical detection, a change in the probe design will improve the detection performance in the future.

Although noncontact detection methods can avoid a random measurement error, the experimental setup requires a large footprint. Noncontact detecting sensors are typically used in applications where fast displacement changes are required, no forces can be exerted on the measurement object, highly sensitive surfaces do not allow any contact, or longer sensor service life is required. However, noncontact sensors are not widely used for *in vivo* measurement on soft tissue because of its high cost and low measurement accuracy.

The proposed methods showed possibility to improve the conventional method in lymphedema evaluation in animal study. The methods facilitate the extraction of longitudinal section-specific information, which can be an important clue in lymphatics. Although there are several limitations in the physical detecting method such as skin deformation and the linear elastic range, the differences between the visual detecting method and the physical detecting method can be combined to take another advantage. For example, a spring in the probe can be changed to another spring that has different spring constant. If a known force is applied to the skin tissue by a physical contact-type probe, differences between geometric information obtained from visual detection and physical detection can be merged to define a novel stage classification method of lymphedema. In contrast, the novel methods are still based on the assumption that the tail is a perfect circle at every cross section. To overcome this limitation, the number of measuring planes should be increased in both methods.

Acknowledgments

This work was supported by the National Research Foundation of Korea (NRF) Grant funded by the Korean Government (MSIP) (No. NRF-2016R1A5A1938472). This study was supported by Fund of Biomedical Research Institute, Chonbuk National University Hospital.

Author Disclosure Statement

No competing financial interests exist.

References

1. Mortimer PS. Therapy approaches for lymphedema. Angiology 1997; 48:87–91.
2. Cheng M-H, Chang DW, Patel KM. Laboratory study of lymphedema. In: *5. Principles and Practice of Lymphedema Surgery.* Amsterdam: Elsevier; 2015:32–39.
3. Kanter MA, Slavin SA, Kaplan W. An experimental model for chronic lymphedema. Plast Reconstr Surg 1990; 85:573–580.
4. Shin WS, Szuba A, Rockson SG. Animal models for the study of lymphatic insufficiency. Lymphat Res Biol 2003; 1:159–169.
5. Tobbia D, Semple J, Baker A, et al. Lymphedema development and lymphatic function following lymph node excision in sheep. J Vasc Res 2009; 46:426–434.
6. Cheung L, Han J, Beilhack A, et al. An experimental model for the study of lymphedema and its response to therapeutic lymphangiogenesis. Biodrugs 2006; 20:363–370.
7. Wang GY, Zhong SZ. A model of experimental lymphedema in rats' limbs. Microsurgery 1985; 6:204–210.
8. Lee-Donaldson L, Witte M, Bernas M, et al. Refinement of a rodent model of peripheral lymphedema. Lymphology 1999; 32:111–117.
9. Oashi K, Furukawa H, Oyama A, et al. A new model of acquired lymphedema in the mouse hind limb: A preliminary report. Ann Plast Surg 2012; 69:565–568.
10. Rutkowski JM, Moya M, Johannes J, et al. Secondary lymphedema in the mouse tail: Lymphatic hyperplasia, VEGF-C upregulation, and the protective role of MMP-9. Microvasc Res 2006; 72:161–171.
11. Chang T-C, Uen Y-H, Chou C-H, et al. The role of cyclooxygenase-derived oxidative stress in surgically induced lymphedema in a mouse tail model. Pharm Biol 2013; 51:573–580.
12. Ho Joong Jeong, Ki Hun Hwang, Sim Y-J, Ghi Chan Kim, Kim Y-O, Baek S-M. The study of animal model of lymphedema using the mouse tail. Kosin Med J 2012; 27:141–149.
13. Onishi T, et al. Topical bFGF improves secondary lymphedema through lymphangiogenesis in a rat tail model. Plast Reconstr Surg Glob Open 2014; 2:e196.
14. Sommer T, Buetter M, Bruns F, et al. Quantification of lymphedema in a rat model by 3D-active contour segmentation by magnetic resonance imaging. Lymphat Res Biol 2012; 10:25–29.
15. Yasumura S, Harrison JE. In vivo body composition studies: Recent advances. New York: Plenum Press; 1990.
16. Jun H, Lee JY, Kim JH, Noh M, Kwon TW, Cho YP, et al. Modified mouse models of chronic secondary lymphedema: Tail and hind limb models. Ann Vasc Surg 2017; 43: 288–295.
17. Ballard DH, Brown CM. *Computer Vision.* Englewood Cliffs, NJ: Prentice Hall; 1982.
18. Sonka M, Hlavac V, Boyle R. *Image Processing, Analysis, and Machine Vision*. Toronto, ON: Thomson; 2008.
19. Canny J. A computational approach to edge detection. IEEE Trans Pattern Anal Machine Intell 1986; PAMI-8: 679–698.
20. Lynch LL, Mendez U, Waller AB, Gillette AA, Guillory RJ, 2nd, Goldman J. Fibrosis worsens chronic lymphedema in rodent tissues. Am J Physiol Heart Circ Physiol 2015; 308:H1229–H1236.
21. Frueh FS, Korbel C, Gassert L, Muller A, Gousopoulos E, Lindenblatt N, Giovanoli P, Laschke MW, Menger MD. High-resolution 3D volumetry versus conventional measuring techniques for the assessment of experimental lymphedema in the mouse hindlimb. Sci Rep 2016; 6: 34673.

Address correspondence to:
Kyu-jin Cho, PhD
Biorobotics Laboratory
Department of Mechanical and Aerospace Engineering
Seoul National University
1, Kwanak-ro, Sinrim-dong, Kwanak-ku
Seoul 08826
Republic of Korea

E-mail: kjcho@snu.ac.kr

Downloaded by Seoul National Univ. Medical College from www.liebertpub.com at 12/23/18. For personal use only.